On the quantification of [F-18]MPPF binding to 5-HT1A receptors in the human brain

Passchier, Jan; van Waarde, A; Vaalburg, W; Willemsen, ATM

Published in:
Journal of Nuclear Medicine

Publication date:
2001

On the Quantification of [^{18}F]MPPF Binding to 5-HT$_{1A}$ Receptors in the Human Brain

Jan Passchier, Aren van Waarde, Willem Vaalburg, and Antoon T.M. Willemsen

PET Center, Groningen University Hospital, Groningen; Groningen University Institute for Drug Exploration, Groningen, The Netherlands

Previous studies have shown that 4-(2′-methoxyphenyl)-1-[2′-(*N*-2″-pyridinyl)-*p*-[^{18}F]fluorobenzamido]ethylpiperazine ([^{18}F]MPPF) binds with high selectivity to serotonin (5-HT$_{1A}$) receptors in man. However, in these studies, the calculation of the binding potential (BP, which equals receptor density divided by equilibrium dissociation constant) used a metabolite-corrected arterial input. The aim of this study was to determine whether metabolite correction and arterial sampling are essential for the assessment of BP. **Methods:** Five analytic methods using full datasets obtained from 6 healthy volunteers were compared. In addition, the clinical applicability of these methods was appraised. Three methods were based on Logan analysis of the dynamic PET data using metabolite-corrected and uncorrected arterial plasma input and cerebellar input. The other 2 methods consisted of a simplified reference tissue model and standard compartmental modeling. **Results:** A high correlation was found between BP calculated with Logan analysis using the metabolite-corrected plasma input (used as the reference method for this study) and Logan analysis using either the uncorrected arterial plasma input (r^2 = 0.95, slope = 0.85) or cerebellar input (r^2 = 0.98, slope = 0.91). A high correlation was also found between our reference method and the simplified reference tissue model (r^2 = 0.94, slope = 0.92). In contrast, a poor correlation was observed between our reference method and the standard compartmental model (r^2 = 0.45, slope = 1.59). **Conclusion:** These results indicate that neither metabolite analysis nor arterial sampling is necessary for clinical evaluation of BP in the human brain with [^{18}F]MPPF. Both the Logan analysis method with cerebellar input and the simplified reference tissue method can be applied clinically.

Key Words: serotonin receptor; binding potential; PET; modeling

J Nucl Med 2001; 42:1025–1031

The serotonin (5-HT$_{1A}$) receptor plays an important role in the pathophysiology of a variety of psychiatric and neurodegenerative diseases such as depression, schizophrenia, and dementia (*1–4*). Autoradiography studies have shown changes in the receptor density that may be related to the symptoms that are observed in these disorders (*5–9*). Clearly, the ability to determine receptor binding noninvasively would enhance the prospect of early diagnosis and assessment of disease progression as well as offer a potential way to evaluate therapy and early (phases 1 and 2) drug testing. PET is a unique technique that provides the possibility of imaging and quantifying metabolic processes and receptor binding. Animal studies have shown the selectivity of 4-(2′-methoxyphenyl)-1-[2′-(*N*-2″-pyridinyl)-*p*-[^{18}F]fluorobenzamido]ethylpiperazine ([^{18}F]MPPF) for the 5-HT$_{1A}$ receptor (*10–14*). Studies on volunteers have shown that regional uptake agreed well with known receptor distribution (*14–20*). (The various radioligands for the 5-HT$_{1A}$ receptor have been reviewed (*21*).) Using a metabolite-corrected input function in a Logan analysis (*22*), binding potentials (BPs, which equal receptor density [B_{max}] divided by equilibrium dissociation constant [K_D]) were estimated in several regions from their respective distribution volumes (DVs) (BP $\approx DV_{region}/DV_{cerebellum} - 1$). The resulting apparent BP closely correlated with previous PET studies using [carbonyl-^{11}C]WAY 100635 (*17,18,23–25*) and with ex vivo autoradiography (*26*). Unfortunately, the requirement of arterial sampling and metabolite analyses hampers the clinical applicability of this method.

The aim of this study was to determine whether metabolite correction and arterial sampling are essential for the assessment of BP. Therefore, full datasets obtained from healthy volunteers were analyzed by several methods. In addition, the clinical applicability of the analysis methods was appraised.

MATERIALS AND METHODS

Volunteers

Approval was gained from the medical ethics committee of the Groningen University Hospital for this study. Six volunteers (2 men, 4 women; age range, 19–65 y) were included after written informed consent had been obtained and an independent physician had confirmed their suitability to take part in the study according to the following inclusion and exclusion criteria: age between 18 and 65 y; healthy according to medical examination; no history of neurodegenerative or psychiatric disorders; no use of neuroleptic drugs, sedative drugs, or antidepressants; no use of corticosteroids or agents that suppress adrenal function; and no pregnancy or possibility of pregnancy.

Received Nov. 13, 2000; revision accepted Mar. 5, 2001.

For correspondence or reprints contact: Antoon T.M. Willemsen, PhD, PET Center, Groningen University Hospital, P.O. Box 30001, 9700 RB Groningen, The Netherlands.

Experimental Procedure

Radiochemistry. [^{18}F]MPPF was prepared by nucleophilic substitution of the aromatic nitro group (a comparable method has been described elsewhere (*11,12*)). Quality control was performed using reverse-phase high-performance liquid chromatography (Nova-Pak; Waters, Milford, MA) with the following parameters: 150 × 3.9 mm, acetonitrile/tetrahydrofuran/0.01N NaOAc = 28:6:65, pH 5, retention time (t_R) of [^{18}F]MPPF = 5 min, t_R of the nitro precursor of MPPF = 7 min. The levels of the nitro precursor were << 1 mg/L, and no detectable amounts of WAY-100634 (nonradioactive compound that is formed by hydrolysis of the nitroprecursor during the synthesis, with affinity for both the 5-HT_{1A} and the α_1-adrenergic receptor (*27*)) were observed. The radiochemical purity of the product was >99%.

PET Measurements. PET was performed on an ECAT EXACT HR+ (CTI, Knoxville, TN/Siemens Medical Systems, Inc., Hoffman Estates, IL) with a resolution of 4 to 5 mm full width at half maximum, giving 63 slices with a center-to-center distance of 2.425 mm. The volunteers were positioned in the camera using a head restraint, and a transmission scan was obtained using 3 ^{68}Ge/^{68}Ga rod-sources for consequent attenuation correction of the dynamic PET data. After the transmission scan, the volunteers received an intravenous bolus injection (10 s) of 1,850 MBq [^{15}O]H_2O in 10 mL saline (0.9%). Radioactivity in the brain was measured during 15 min. Eight consecutive frames were acquired. At least 15 min after administration of [^{15}O]H_2O, during which the volunteer remained in the camera, 69 ± 17 MBq [^{18}F]MPPF (specific activity > 110 TBq/mmol at the time of injection) in 10 mL phosphate buffer (Na_3PO_4 = 9.0 mmol/L; Na_2HPO_4 = 1.3 mmol/L; 0.9% saline) at pH 7.4–7.6 with 7%–8% ethanol were administered intravenously over 1 min. Twenty-one consecutive frames were acquired, consisting of six 10-s frames, three 30-s frames, two 60-s frames, two 120-s frames, two 180-s frames, three 300-s frames, and three 600-s frames. Blood samples were taken manually from the radial artery at 30-s intervals for the first 5 min, followed by 6 samples from 10 to 60 min at 10-min intervals, giving a total of 16 samples. After centrifugation, 250-μL samples of plasma were counted in a calibrated γ counter (CompuGamma 1282 CS; LKB-Wallac, Turku, Finland) to obtain the arterial input function. Whole-blood samples (250 μL) were also counted to estimate binding of [^{18}F]MPPF to erythrocytes.

Metabolites. Seven of the 16 arterial plasma samples (1 mL, obtained at 1, 2, 5, 10, 20, 40, and 60 min) were deproteinized with 70% perchloric acid (0.05–0.1 volume) to determine the rate of metabolism. After precipitation of protein by centrifugation, the supernatant was injected onto a Nova-Pak system (150 × 3.6 mm; MeOH/0.1N NH_4HCO_2/Et_3N = 45:55:0.3, flow rate = 1.0 mL/min), and 30 samples were collected during 15 min using a fraction collector. The retention time of the parent compound was 9 min.

Data Analysis

Regions of Interest. The image obtained by summation of the [^{18}F]MPPF frames (5–60 min) was used to determine areas with enhanced uptake, in particular the medial temporal cortex and the insular cortex. In addition, the image obtained by summation of the [^{15}O]H_2O scan (0–3.5 min) was used to obtain anatomic information on areas with moderate uptake, in particular the frontal, cingulate, and lateral temporal cortices. Regions of interest (ROIs) were drawn manually in the transaxial orientation using a contour tool (Clinical Applications Programming Package; CTI). Partial-volume correction was not applied.

BPs. Five methods for the calculation of BP were compared. Three methods were based on Logan analysis of the dynamic PET data for the calculation of DVs using metabolite-corrected and uncorrected arterial plasma input or cerebellar input, from which the BP can be calculated using $BP = DV_{region}/DV_{cerebellum} - 1$ (*21,28*). The other 2 methods consisted of a simplified reference tissue model (*29,30*) and standard compartmental modeling (*23,24,31*). All calculations were performed in MATLAB (The MathWorks, Inc., Natick, MA), with the Logan-based analysis using least squares linear regression and the simplified reference tissue model and standard compartmental modeling using the Levenberg–Marquart optimization algorithm. Kruskal–Wallis nonparametric ANOVA with Bonferroni post hoc multiple comparisons testing was performed to analyze the differences between the various methods (SPSS, version 10; SPSS Inc., Chicago, IL). Two-tailed probability values of <0.05 were considered significant.

RESULTS

Intravenously injected [^{18}F]MPPF was rapidly distributed throughout the brain. ROI-derived time–activity curves showed a rapid decrease of radioactivity in the cerebellum and a slower decrease in target areas (i.e., frontal, cingulate, insular, lateral temporal, and medial temporal cortices). An example of time–activity curves for the cerebellum and the frontal, insular, and medial temporal cortices in a single volunteer is shown in Figure 1A. The corresponding specific binding (calculated by subtraction of the cerebellar time–activity curve from the tissue time–activity curves) is shown in Figure 1B. Tissue-over-cerebellum ratios reached a maximum between 30 and 45 min after injection. Levels

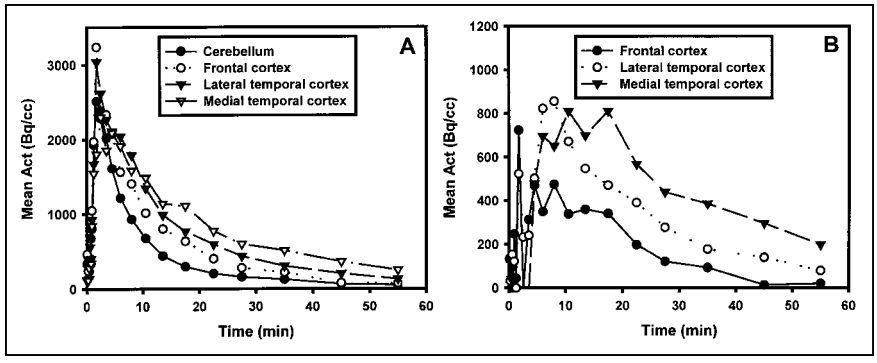

FIGURE 1. Time–activity (Act) curves (A) and corresponding specific binding (B) for several regions in 1 volunteer after administration of 79 MBq [^{18}F]MPPF.

TABLE 1
Calculated BPs for Several Regions Using 5 Methods

Region	Method*				
	1	2	3	4	5
FC	0.64 ± 0.06	0.57 ± 0.08	0.64 ± 0.05	0.49 ± 0.05	0.91 ± 0.40
CC	0.83 ± 0.09	0.71 ± 0.09	0.84 ± 0.12	0.65 ± 0.11	1.23 ± 0.57
INS	1.32 ± 0.24	1.19 ± 0.26	1.29 ± 0.21	1.18 ± 0.21	1.89 ± 1.06
LTC	1.19 ± 0.11	1.05 ± 0.14	1.16 ± 0.13	1.08 ± 0.21	1.75 ± 0.47†
MTC	2.02 ± 0.27	1.72 ± 0.27	1.92 ± 0.18	1.77 ± 0.23	3.24 ± 1.54†

*Logan (*22*) analysis using metabolite-corrected arterial input (method 1), uncorrected arterial input (method 2), or cerebellar time–activity curve input (method 3); simplified reference tissue model (method 4) (*28*); and standard compartmental modeling (method 5).

†Significantly different ($P < 0.05$) compared with method 1.

FC = frontal cortex; CC = cingulate cortex; INS = insular cortex; LTC = lateral temporal cortex; MTC = medial temporal cortex.

Data are listed as mean ± SD ($n = 6$).

were 2 for the frontal and cingulate cortices, 3–4 for the insular and lateral temporal cortices, and 6 for the medial temporal cortex. As shown previously, [^{18}F]MPPF rapidly cleared from plasma and was subject to a high rate of metabolism, resulting in approximately 1% parent compound in plasma after 10 min (*18*).

To calculate BP, ROI-derived time–activity curves were used to determine the DVs. The resulting BPs obtained for the 5 methods are displayed in Table 1. The 3 Logan analyses (i.e., using metabolite-corrected arterial input, uncorrected arterial input, or cerebellar input) gave similar results. Comparison of the ROI-derived BP obtained for each volunteer using the second and third methods with the first method (used as the reference method for this study) showed an excellent correlation ($r^2 = 0.95$, slope = 0.85, and $r^2 = 0.98$, slope = 0.91, respectively; Figs. 2A and 2B). The simplified reference tissue method, using the cerebellum as reference tissue, also gave results that closely matched our reference method ($r^2 = 0.94$, slope = 0.92; Fig. 2C). Compartmental modeling failed to generate reliable values for k_3 and k_4, leading to BPs that correlated poorly with our reference method ($r^2 = 0.45$, slope = 1.59; Fig. 2D). Statistical analysis showed that only the standard compartmental modeling method resulted in significantly different BP results compared with the other methods. In particular, compared with our reference method, BP in the lateral and temporal cortices were significantly higher when calculated with compartmental modeling.

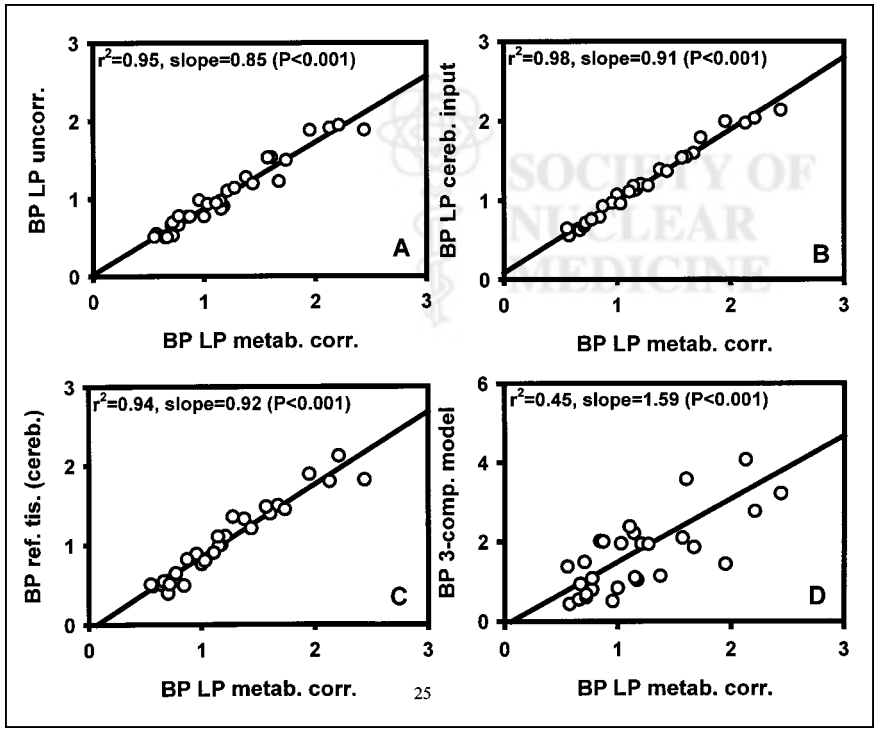

FIGURE 2. Comparison of BPs obtained by Logan analysis (*21*) using metabolite-corrected arterial input (BP LP metab. corr.) with uncorrected arterial input (BP LP uncorr.) (A), with cerebellar input (BP LP cereb. input) (B), with simplified reference tissue method (BP ref. tis. [cereb.] (*27*)) (C), and with compartmental modeling (BP 3-comp. model) (D).

To assess if the similarity between ROI-derived BPs in the selected target areas could be translated to the entire brain, we performed pixel-by-pixel parametric imaging for the Logan analysis using either the metabolite-corrected or uncorrected arterial input and the reference tissue model. In Figure 3, the images obtained by summation of the frames (5–60 min) (Fig. 3A) can be compared with the resulting parametric images at the level of the basal ganglia and at the level of the medial temporal cortex (Figs. 3B–3D).

DISCUSSION

As shown previously (*15–18*), [^{18}F]MPPF is rapidly taken up in the brain and then clears quickly from the cerebellum and more slowly from target areas (Fig. 1A). Moreover, the distribution of [^{18}F]MPPF agrees well with known 5-HT_{1A} receptor localization in the brain (Fig. 3A) (*19,20,26,32*). In previous studies, BPs for [^{18}F]MPPF were calculated through Logan analysis using the metabolite-corrected arterial input function (*17,18,22*). A drawback of this method is that it requires both arterial sampling and metabolite analysis. The literature has shown that the cerebellum of adult primates contains few or no 5-HT_{1A} receptors (*19,26,32,33*); therefore, use of this region as a reference may be possible because the radioactivity that appears in the cerebellum after injection represents the free fraction of the radioligand in the brain.

In this study, 5 different methods for the calculation of BP were compared to determine whether metabolite correction and arterial sampling are essential for the assessment of BP. In addition, the clinical applicability of these methods was appraised. Obviously, the time–activity curves and, therefore, the resulting DVs and BP are susceptible to inter- and intraobserver variability and to partial-volume effects. However, these will not influence the comparison of different methods as presented here. The Logan method using metabolite-corrected arterial plasma input has proven effective for the assessment of DV for several radioligands (*22,34,35*) and has shown excellent fits in preliminary studies with [^{18}F]MPPF (*18*). In addition, we observed severe problems in the assessment of BP through compartmental fitting. Therefore, we chose the Logan-based method (*17*) as the reference for this study. All the methods used in this study neglect cerebral blood volume because it is generally small (3%–5%) (*36*).

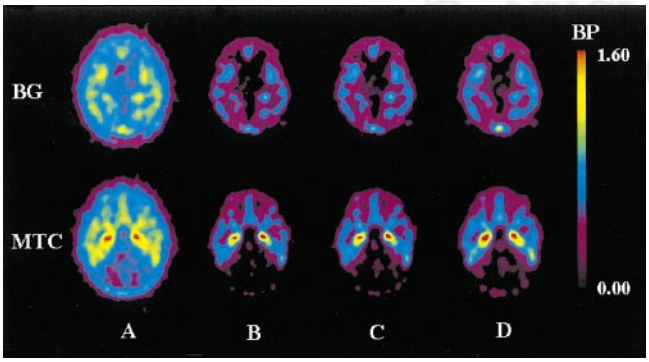

FIGURE 3. Comparison of frame summation (5–60 min) (A) with results of pixel-by-pixel–based parametric imaging of Logan analysis using metabolite-corrected arterial input (B), cerebellar input (C) (*21*), and simplified reference tissue method (D) (*27*) at level of basal ganglia (BG) and medial temporal cortex (MTC).

As a first approach, metabolite correction of the plasma input was dismissed. Considering the fast metabolism of MPPF, this simplification changes the apparent DVs (DV*) of both the target and the reference tissue considerably. However, we determined that omitting the metabolite correction of the plasma input has little effect on BP (Table 1; Fig. 2A). These findings can be predicted given a set of model assumptions. Basically, both target and reference DVs are affected equally by the metabolite correction. As a consequence, the BP, which is based on the ratio of the DVs, is independent of the metabolite analysis. A similar conclusion can be drawn for the use of the cerebellar time–activity data as the apparent plasma input (Appendix). In this special case, the DV* of the cerebellum naturally reduces to unity and the determination of the BP can be simplified to $BP = DV^*_{target} - 1$.

In this study, we assumed that the plasma metabolites do not cross the blood–brain barrier. Data on rats confirm this assumption (*37*). Both in our reference method and in the first 2 simplifications, the DVs for the free tracer, K_1/k_2 and K_1'/k_2', respectively, are assumed to be identical in both target and reference tissue. This assumption is also made in the simplified reference tissue model. Also, the possibility has been shown that direct calculation of the DV ratio, from which the BP was calculated, by applying the cerebellum time–activity data as input may result in a bias (*28*). Consequently, estimation of BP by either the Logan-based methods or the simplified reference tissue model may be biased in comparison with direct assessment of BP through the equation $BP = B_{max}/K_D$. To use the term *apparent BP* for the BP derived from the Logon-based methods or the simplified reference tissue model would therefore be more appropriate.

Direct assessment of BP through compartmental modeling resulted in a poor match with our reference method (Table 1; Fig. 2D). This observation can be explained from the poor quality of the values obtained for k_3 and k_4. A similar effect was found in the assessment of [^{11}C]raclopride binding to the dopamine receptors (*29*), indicating that for the quantification of [^{18}F]MPPF binding to 5-HT_{1A} receptors, a method that does not depend on calculation of individual rate constants is desirable. Considering the excellent correlation between BP determined using either our reference method or the simplified methods (Figs. 2A–2C), we can conclude that deviations from the model assumption actually have only a small effect on BP. The excellent correlation of our reference method with both the Logan analysis using cerebellar input and the simplified reference tissue method, combined with the fact that for these 2

methods, arterial sampling and metabolite analysis are not necessary, show that of the 5 methods tested, these are most suited for clinical assessment of 5-HT_{1A} BP. One further alternative for the estimation of BP is, of course, the use of the target-to-cerebellum ratio. Previously, this ratio, corrected for body weight, was shown to correlate strongly ($r^2 = 0.92$) with BP (*18*). However, the deviations were somewhat larger when compared with the current results. Nevertheless, for purely clinical applications, this approach might be developed further and could potentially reduce scanning time to 5–10 min.

CONCLUSION

Using 5 methods for the assessment of BP for [^{18}F]MPPF in the human brain, we have shown that neither arterial sampling nor metabolite analysis is needed. Use of cerebellar input in the Logan analysis or of the cerebellum as reference tissue in the simplified reference tissue model provides results similar to those of Logan analysis with metabolite-corrected arterial plasma input. Considering the excellent correlation between our reference method and both the simplified Logan analysis and the simplified reference tissue model, we can conclude that the two are equivalent for the determination of BP. These simplified methods are readily applicable clinically.

APPENDIX

Determination of BP by DV

Consider the standard 2-compartment model for a reference region without specific binding, with K_1 and k_2 the rate constants for the transfer of the ligand from plasma to reference region and vice versa. For the target area, specific binding is added, with rate constants k_3 and k_4 describing the association and dissociation, respectively, of the ligand with the receptor. In both models, nonspecifically bound activity is considered negligible or in transient equilibrium with free ligand. In the latter case, the BP will be biased; however, this bias is only a scaling factor provided that the level of nonspecific binding is relatively constant. Using metabolite-corrected arterial input, the amount of radioactivity present in a reference region as a function of time is given by:

$$\frac{dC_r}{dt} = K_1'C_p(t) + k_2'C_r(t), \qquad \text{Eq. 1A}$$

where $C_r(t)$ is activity in the reference region ($Bq \cdot mL^{-1}$), $C_p(t)$ is the metabolite-corrected arterial plasma concentration ($Bq \cdot mL^{-1}$), K_1' is the rate constant for transfer from the plasma to the reference region (min^{-1}), and k_2' is the rate constant for transfer from the reference region to the plasma (min^{-1}). The DV for this region is then defined at equilibrium ($dC_r/dt = 0$) and given by:

$$DV_{reference} = \frac{C_{pet}(t)}{C_p(t)} = \left.\frac{C_r(t)}{C_p(t)}\right|_{equilibrium} = \frac{K_1'}{k_2'}, \qquad \text{Eq. 2A}$$

assuming that the cerebral blood volume is negligible (generally small [3%–5%] (*36*)). For the target area where specific binding occurs, the free (i.e., not receptor bound) and bound fractions are given by:

$$\frac{dC_f}{dt} = K_1C_p(t) - (k_2 + k_3)C_f(t) + k_4C_b(t) \text{ and} \qquad \text{Eq. 3A}$$

$$\frac{dC_b}{dt} = k_3C_f(t) - k_4C_b(t), \qquad \text{Eq. 4A}$$

where C_f is the free fraction of radioactivity in target tissue ($Bq \cdot mL^{-1}$), C_b is the receptor-bound fraction of radioactivity in target tissue ($Bq \cdot mL^{-1}$), K_1 is the rate transfer constant from the plasma to the free compartment (min^{-1}), k_2 is the rate transfer constant from the free to the bound compartment (min^{-1}), k_3 is the rate transfer constant from the free to the bound compartment (min^{-1}), and k_4 is the rate transfer constant from the bound to the free compartment (min^{-1}). At equilibrium these equations yield:

$$C_b(t) = \frac{k_3}{k_4}C_f(t) \text{ and} \qquad \text{Eq. 5A}$$

$$C_f(t) = \frac{K_1}{k_2}C_p(t), \qquad \text{Eq. 6A}$$

and the DV is given by:

$$DV_{target} = \left.\frac{C_{pet}(t)}{C_p(t)}\right|_{equilibrium} = \frac{C_f(t) + C_b(t)}{C_p(t)} = \frac{K_1}{k_2}\left(1 + \frac{k_3}{k_4}\right). \qquad \text{Eq. 7A}$$

Assuming that $(K_1/k_2) \equiv (K_1'/k_2')$, the BP can then be calculated by:

$$BP = \frac{DV_{target}}{DV_{reference}} - 1 = \frac{K_1/k_2(1 + k_3/k_4)}{K_1'/k_2'} - 1 = \frac{k_3}{k_4}. \qquad \text{Eq. 8A}$$

We found that after 10 min, the Logan curve could be well approximated by a straight line. Consequently, in practice, DVs and BPs can be determined using Logan analysis, even though the overall system is not in equilibrium (*22*).

Dismissal of Metabolite Correction

When uncorrected arterial plasma is used as the input function, the apparent DV in free tissue is given by:

$$DV^u_{reference} = \frac{C_r(t)}{C^u_p(t)} = \frac{K_1'}{k_2'}\frac{C_p(t)}{C^u_p(t)}, \qquad \text{Eq. 9A}$$

where $C^u_p(t)$ is the uncorrected arterial plasma concentration ($Bq \cdot mL^{-1}$). For the target tissue, the apparent DV is now given by:

$$DV^{u}_{target} = \frac{C_{pet}(t)}{C^{u}_{p}(t)} = \frac{C_f(t) + C_b(t)}{C^{u}_{p}(t)} = \frac{K_1}{k_2}\left(1 + \frac{k_3}{k_4}\right)\frac{C_p(t)}{C^{u}_{p}(t)}. \quad \text{Eq. 10A}$$

Again assuming that $(K_1/k_2) \equiv (K_1'/k_2')$, calculation of BP then leads to the well-known solution:

$$BP = \frac{DV_{region}}{DV_{reference}} - 1 = \frac{K_1/k_2(1 + k_3/k_4)(C_p(t)/C^{u}_{p}(t))}{K_1'/k_2'(C_p(t)/C^{u}_{p}(t))} - 1 = \frac{k_3}{k_4}, \quad \text{Eq. 11A}$$

showing that the determination of BP based on uncorrected plasma data (Eq. 11A) is identical to the determination of BP based on metabolite-corrected plasma data (Eq. 8A).

Cerebellar Time–Activity Data as Apparent Plasma Input

When, instead of the metabolite-corrected plasma input function, the time–activity curve of a reference region (e.g., cerebellum) is used as the input function, the apparent DV in this region is clearly normalized to 1 ($DV^{c}_{reference}$). Substituting $C_p(t)$ with $C_r(t)$ in Eq. 7A gives:

$$DV^{c}_{target} = \frac{C_{pet}(t)}{C_r(t)} = \frac{C_f(t) + C_b(t)}{C_r(t)} = \frac{K_1/k_2(1 + k_3/k_4)C_p(t)}{K_1'/k_2'C_p(t)} = 1 + \frac{k_3}{k_4}, \quad \text{Eq. 12A}$$

from which BP can be obtained by:

$$BP = DV^{c}_{target} - 1, \quad \text{Eq. 13A}$$

showing that the determination of BP based on a reference region (Eq. 13A) is identical to the determination of BP based on the metabolite-corrected plasma data (Eq. 8A).

REFERENCES

1. Bowen DM, Najlerahim A, Procter AW, et al. Circumscribed changes of the cerebral cortex in neuropsychiatric disorders of later life. *Proc Natl Acad Sci USA.* 1989;86:9504–9508.
2. Cowen PJ. Serotonin receptor subtypes in depression: evidence from studies in neuroendocrine regulation. *Clin Neuropharmacol.* 1993;16(suppl 3):S6–S18.
3. Robinson DS, Alms DR, Shrotriya RC, et al. Serotonergic anxiolytics and treatment of depression. *Psychopathology.* 1989;22(suppl 1):27–36.
4. Zifa E, Fillion G. 5-Hydroxytryptamine receptors. *Pharmacol Rev.* 1992;44:401–458.
5. Burnet PW, Eastwood SL, Harrison PJ. 5-HT_{1A} and 5-HT_{2A} receptor mRNAs and binding site densities are differentially altered in schizophrenia. *Neuropsychopharmacology.* 1996;15:442–455.
6. Burnet PW, Eastwood SL, Harrison PJ. [^{3}H]WAY-100635 for 5-HT_{1A} receptor autoradiography in human brain: a comparison with [^{3}H]8-OH-DPAT and demonstration of increased binding in the frontal cortex in schizophrenia. *Neurochem Int.* 1997;30:565–574.
7. Hashimoto T, Nishino N, Nakai H, et al. Increase in serotonin 5-HT_{1A} receptors in prefrontal and temporal cortices of brains from patients with chronic schizophrenia. *Life Sci.* 1991;48:355–363.
8. Stockmeier CA, Shapiro LA, Dilley GE, et al. Increase in serotonin-1A autoreceptors in the midbrain of suicide victims with major depression: postmortem evidence for decreased serotonin activity. *J Neurosci.* 1998;18:7394–7401.
9. Sumiyoshi T, Stockmeier CA, Overholser JC, et al. Serotonin$_{1A}$ receptors are increased in postmortem prefrontal cortex in schizophrenia. *Brain Res.* 1996;708: 209–214.
10. Kung HF, Stevenson DA, Zhuang ZP, et al. New 5-HT1A receptor antagonist: [^{3}H]p-MPPF. *Synapse.* 1996;23:344–346.
11. Shiue CY, Shiue GG, Mozley PD, et al. P-[^{18}F]-MPPF: a potential radioligand for PET studies of 5-HT_{1A} receptors in humans. *Synapse.* 1997;25:147–154.
12. Le Bars D, Lemaire C, Ginovart N, et al. High-yield radiosynthesis and preliminary in vivo evaluation of p-[^{18}F]MPPF, a fluoro analog of WAY-100635. *Nucl Med Biol.* 1998;25:343–350.
13. Passchier J, Van Waarde A, Doze P, et al. Regional distribution of two 5-HT_{1A} receptor ligands in rat brain and effect of Pgp modulation [abstract]. *J Nucl Med.* 1999;40(suppl):263P.
14. Ginovart N, Hassoun W, Le Bars D, et al. In vivo characterization of p-[^{18}F]MPPF, a fluoro analog of WAY-100635 for visualization of 5-HT_{1A} receptors. *Synapse.* 2000;35:192–200.
15. Passchier J, Van Waarde A, Pieterman RM, et al. Delineation of serotonin (5-HT)$_{1A}$ receptors in human brain with [^{18}F]MPPF [abstract]. *J Nucl Med.* 1999;40(suppl):29P.
16. Plenevaux A, Lemaire C, Salmon E, et al. 5-HT_{1A} receptors visualization with p-[^{18}F]MPPF in healthy volunteers [abstract]. *J Labelled Cpd Radiopharm.* 1999;42(suppl 1):S60–S62.
17. Passchier J, Van Waarde A, Pieterman RM, et al. Quantitative imaging of 5-HT_{1A} receptor binding in healthy volunteers with [^{18}F]p-MPPF. *Nucl Med Biol.* 2000; 27:473–476.
18. Passchier J, Van Waarde A, Pieterman RM, et al. *In vivo* delineation of serotonin (5-HT)$_{1A}$ receptors in human brain with [^{18}F]MPPF. *J Nucl Med.* 2000;41:1830–1835.
19. Burnet PW, Eastwood SL, Lacey K, et al. The distribution of 5-HT_{1A} and 5-HT_{2A} receptor mRNA in human brain. *Brain Res.* 1995;676:157–168.
20. Pazos A, Probst A, Palacios JM. Serotonin receptors in the human brain. III. Autoradiographic mapping of serotonin-1 receptors. *Neuroscience.* 1987;21:97–122.
21. Passchier J, van Waarde A. Visualisation of serotonin-1A (5-HT1A) receptors in the central nervous system. *Eur J Nucl Med.* 2001;28:113–129.
22. Logan J, Fowler JS, Volkow ND, et al. Graphical analysis of reversible radioligand binding from time-activity measurements applied to [N-^{11}C-methyl]-(−)-cocaine PET studies in human subjects. *J Cereb Blood Flow Metab.* 1990;10: 740–747.
23. Farde L, Ito H, Swahn CG, et al. Quantitative analyses of carbonyl-carbon-11-WAY-100635 binding to central 5-hydroxytryptamine-1A receptors in man. *J Nucl Med.* 1998;39:1965–1971.
24. Gunn RN, Sargent PA, Bench CJ, et al. Tracer kinetic modeling of the 5-HT_{1A} receptor ligand [*carbonyl*-^{11}C]WAY-100635 for PET. *Neuroimage.* 1998;8:426–440.
25. Ito H, Halldin C, Farde L. Localization of 5-HT_{1A} receptors in the living human brain using [*carbonyl*-^{11}C]WAY-100635: PET with anatomic standardization technique. *J Nucl Med.* 1999;40:102–109.
26. Dillon KA, Gross-Isseroff R, Israeli M, et al. Autoradiographic analysis of serotonin 5-HT_{1A} receptor binding in the human brain postmortem: effects of age and alcohol. *Brain Res.* 1991;554:56–64.
27. Pike VW, McCarron JA, Lammertsma AA, et al. Exquisite delineation of 5-HT_{1A} receptors in human brain with PET and [*carbonyl*-^{11}C]WAY-100635. *Eur J Pharmacol.* 1996;301:R5–R7.
28. Logan J, Fowler JS, Volkow ND, et al. Distribution volume ratios without blood sampling from graphical analysis of PET data. *J Cereb Blood Flow Metab.* 1996;16:834–840.
29. Lammertsma AA, Bench CJ, Hume SP, et al. Comparison of methods for analysis of clinical [^{11}C]raclopride studies. *J Cereb Blood Flow Metab.* 1996;16:42–52.
30. Lammertsma AA, Hume SP. Simplified reference tissue model for PET receptor studies. *Neuroimage.* 1996;4:153–158.
31. Huang SC, Barrio JR, Phelps ME. Neuroreceptor assay with positron emission tomography: equilibrium versus dynamic approaches. *J Cereb Blood Flow Metab.* 1986;6:515–521.
32. Hall H, Lundkvist C, Halldin C, et al. Autoradiographic localization of 5-HT_{1A} receptors in the post-mortem human brain using [^{3}H]WAY-100635 and [^{11}C]way-100635. *Brain Res.* 1997;745:96–108.
33. del Olmo E, Diaz A, Guirao-Pineyro M, et al. Transient localization of 5-HT_{1A} receptors in human cerebellum during development. *Neurosci Lett.* 1994;166: 149–152.
34. Petit-Taboué MC, Landeau B, Osmont A, et al. Estimation of neocortical sero-

tonin-2 receptor binding potential by single-dose fluorine-18-setoperone kinetic PET data analysis. *J Nucl Med.* 1996;37:95–104.
35. Wienhard K. Modelisation: application to the D_2 receptors. In: Baron JC, Comar D, Farde L, et al., eds. *Brain Dopaminergic Systems: Imaging with Positron Tomography*. Dordrecht, The Netherlands: Kluwer Academic Publishers; 1991: 85–95.
36. Phelps ME, Huang SC, Hoffman EJ, et al. Validation of tomographic measurement of cerebral blood volume with C-11-labeled carboxyhemoglobin. *J Nucl Med.* 1979;20:328–334.
37. Plenevaux A, Aerts J, Lemaire C, et al. Evaluation of p-[F-^{18}]MPPF, 5-HT_{1A} antagonist, in rats: tissue distribution, autoradiography and metabolism [abstract]. *J Nucl Med.* 1997;38(suppl):56P.